Arch. Metall. Mater. **66** (2021), 1, 273-279

DOI: 10.24425/amm.2021.134785

M. WĘDRYCHOWICZ[1]*, A.W. BYDAŁEK[1,2], P. MIGAS[3], T. SKRZEKUT[4], P. NOGA[4], P. MADEJ[5], A. KAŁASZNIKOW[1]

THE EFFECT OF ADDING IRON POWDER FROM PLASMA CUTTING ON THE MICROSTRUCTURE, MECHANICAL PROPERTIES OF THE COMPOSITE BASED ON ALUMINUM POWDER MATRIX MADE USING POWDER METALLURGY

The paper presents the results of research on the effect of added iron powder from plasma cutting on the mechanical properties and structure of a composite rod based on aluminum powder. The iron powder came from plasma cutting of steel elements and was handed over by the enterprise "AK Anatol" from Żary. One of the ways to dispose of it is to use it as a filler in aluminum composite rods. Research shows that Fe can be distributed in aluminum evenly, and increase in mechanical properties is achieved at the expense of only a slight increase in density. The proposed system does not reduce the amount of waste produced by plasma cutting but finds a use for some of it. The sintering point of the powder required a strongly reducing atmosphere ($P_{O_2} < 10^{-50}$ atm) which seems virtually unachievable under laboratory conditions. The reinforcing mechanism is related to the fragmentation of the matrix aggregate particles and the uniform distribution of Fe particles in the aluminum matrix.

Keywords: Al-Fe composite, iron powder, plasma cutting, aluminum matrix composites, powder metallurgy, mechanical properties

1. Introduction

Dust in steelmaking primarily contains 80% iron, while the remaining components are metal oxides, mainly aluminum. The speed of plasma cutting has a significant impact on the amount of iron dust generated. It is estimated that the amount of iron dust generated during cutting is approx. 0.0175 g/s with an anode diameter of 1 mm [1-2].

Changes in the location of steel dust generation are caused by changes in the distribution of current density and temperature in the arch. The largest loss of iron mass according to the model is found in the immediate vicinity of the anode and it increases over time. The type and quantity of dust generated largely depends on the type of material being cut and the electrodes used [3]. The amount of dust emission is determined based on literature indicators or on the type of steel welded. An example of emission indicators is included in the study [4] Emission of Fume, Nitrogen Oxides and Noise in Plasma Cutting of Stainless and Mild Steel, and some of them are included in Tab. 1.

TABLE 1

Dust emission in plasma cutting for stainless and mild steel [4]

Material, thickness	Dry (g/min)	Semi-dry (g/min)	Wet (g/min)
Mild steel, 8 mm	20-26	2.0-4.0	0.1-0.4
Stainless steel, 8 mm	30-40	3.6-4.6	0.2-0.5
Stainless steel, 35 mm	1.8-3.4	0.1-0.3	0.02

The amount of dust generated in 8 mm mild steel and 8 mm stainless steel is virtually the same [5-7]. In 35 mm stainless, the emission of steel dust is ten times smaller; the study authors note that the cutting speed is also ten times smaller [8-9]. The content of chemical compounds in mild steel ranges from: 67-73% Fe, 2%-10% Mn and Cu, 1.4% Cr, Ni, and Mo, which are undetectable in most samples. In the case of stainless steel, the iron content ranges from 38%-44% Fe, 12%-20% Cr, 4%-8% Ni.

Due to their lightness and excellent mechanical and tribological properties, composites based on an aluminum matrix are

[1] UNIVERSITY OF ZIELONA GÓRA, FACULTY OF MECHANICAL ENGINEERING, 4 PROF. Z. SZAFRANA STR., 65-516 ZIELONA GÓRA, POLAND
[2] WEST POMERANIAN UNIVERSITY OF TECHNOLOGY IN SZCZECIN, FACULTY OF MARITIME TECHNOLOGY AND TRANSPORT, AL. PIASTÓW 41, 71-065 SZCZECIN AL. PIASTÓW 41, 71-065 SZCZECIN
[3] AGH UNIVERSITY OF SCIENCE AND TECHNOLOGY, FACULTY OF METALS ENGINEERING AND INDUSTRIAL COMPUTER SCIENCE, AL. MICKIEWICZA 30, 30-059 KRAKÓW, POLAND
[4] AGH UNIVERSITY OF SCIENCE AND TECHNOLOGY, FACULTY OF NON-FERROUS METALS, AL. MICKIEWICZA 30, 30-059 KRAKÓW, POLAND
[5] ŁUKASIEWICZ RESEARCH NETWORK-INSTITUTE OF NON-FERROUS METALS, PYROMETALLURGY DEPARTMENT, 5 SOWIŃSKIEGO STR., 44-100 GLIWICE, POLAND

* Corresponding author: mwedrychowicz@uz.zgora.pl

among the most desirable engineering materials in the category of metal matrix composites [10-12]. The optimal properties of the composite in an aluminum matrix depend on the appropriate selection of the reinforcement phase and the manufacturing technique. One of the most frequently used methods of making the composite in an aluminum matrix is powder metallurgy [13-16]. It is used due to its low processing costs as well as the ease and accuracy of obtaining geometrically complex components [14-16]. The main parameters of manufacture are powder compaction under externally applied pressure and sintering, and these parameters in turn affect the density of the final product. Increased strength of Al-Fe composites can be achieved by increasing the solubility of Fe solids in Al using non-equilibrium techniques [17-21]. Studies on aluminum powder composites rely on their sintering in the liquid phase or sintering the Fe powder with its high content, i.e. over 20% [22]. Therefore, this paper raises research on developing a method for thickening and sintering the Al-rich Al-Fe binary system, in order to determine the optimal effect of iron content on the physical and mechanical properties of aluminum powder composites.

2. Materials and methods

2.1. Composite preparation

Research on the use of steel dust, S235JR grade unalloyed structural steel was used as a composite filler, made in accordance with the applicable standard EN 10025-2-04, cut in the form of a standard sheet 8 mm thick. The chemical composition of steel dust is shown in Tab. 2.

TABLE 2

Chemical composition of steel dust-
(particle size >200 μm)

Ingredient	[%]
C	2.2
Si	0.33
Mn	1.05
S	0.1
Zn	0.81
Mo	0.24
Fe	56
O	35
Other	4.27

The Iron powder was collected from the plasma cutting process carried out at "AK Anatol" using a WPA-6000 Compact plasma torch, which included: a CNC table, a plasma and gas torch, a ForCUT 133 WDM plasma source, an air dryer, air filters the dust was collected on, and a SMART CNC control program. The starting material for the tests was aluminum powder that was the matrix for the composite and iron powder. Probably, the elevated carbon concentration is a result of high processing temperature with the initial crystallizing outer layer of metal make good conditions of carbon diffusion from the deeper layer of the material to the inner layer of the melting zone.

TABLE 3

Parameters for plasma cutting

Intensity [A]	80
Thickenss of steel [mm]	4
Torch height [mm]	3
Gas pressure – helium [bar]	5.8
Cutting speed [mm/min]	2520

Analysis of the chemical composition of iron powder was carried out using an X-ray fluorescence spectrometer with energy dispersion type: Mini-Pal with an analytical area from Na to U, fitted with Rh lamp with a voltage range from 4 to 30 kV. The measurements were carried out at 298K, in a helium atmosphere, for 100s. The laboratory mixing device, according to the TURBULA concept, was used to homogenize the tested samples: 210 g aluminum powder with 4.2 g iron powder (2%) and 210 g aluminum powder with 10.5 g iron powder (5%). The structure of clean, compressed aluminum powder is a diverse one, containing both small cavities with dimensions of 4-6 μm (approx. 60% of volume) and large, heavily fragmented cavities with dimensions of 8-12 μm (approx. 40% of volume). In samples containing 2% iron powder, these aggregations have a size of about 2-8 μm, while those containing 5% iron powder have aggregations that are similar in size 4-10 μm. The homogenisation procedure was carried out for an hour. Then the powder was pressed on a hydraulic press at a maximum piston pressure of 100 tf. The material obtained from compression in the form of a capsule weighing 30 g of the sample was introduced into the cylindrical chamber. The piston pressure in the chamber was 30 tf.

During the pressing procedure, seven slats (Fig. 1) with a diameter of 38 mm and a height of 10 mm were obtained. These samples were then extruded in parallel at 400°C at a speed of 3 mm / s. Rods with a diameter of 8 mm were obtained (Figs. 4,5).

Fig. 1. An example of sample shape (diameter 38 mm) made by extrusion method of aluminum powder with the addition of 2% iron powder at 400°C, and a stack of samples for extruding bars (right picture)

The mechanical properties were determined using a uniaxial tensile test (Zwick / Roel Z050) at ambient temperature in accordance with EN ISO 6892-1. The microstructural observations were carried out using the Hitachi SU-70 scanning electron

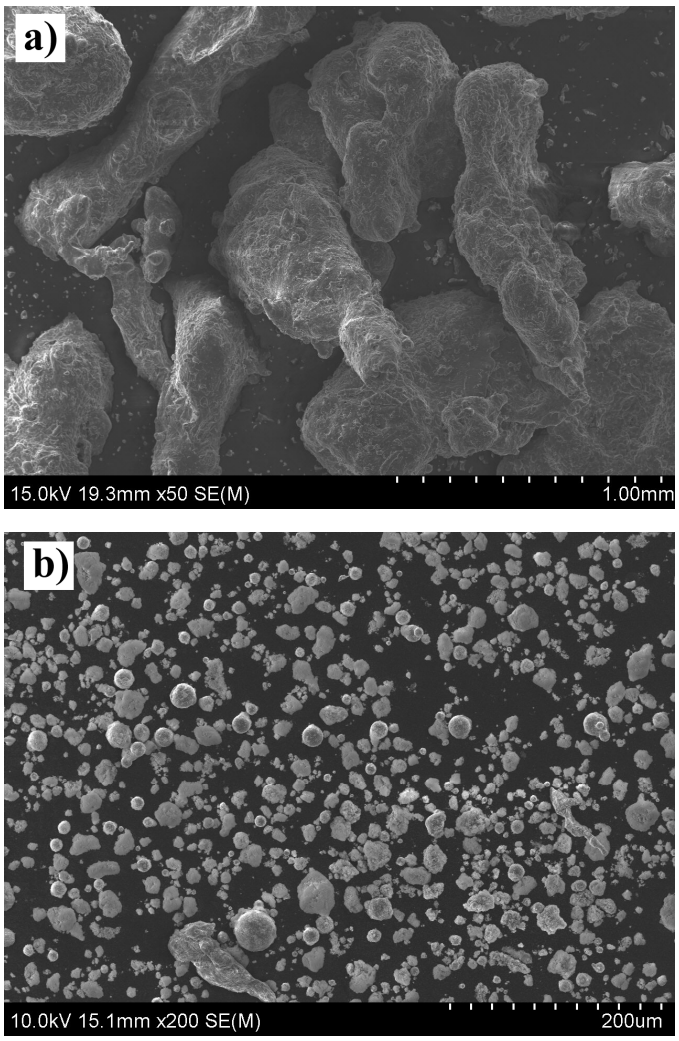

Fig. 2. SEM micrographs of elemental powders of aluminum (a) and iron (b)

microscope. X-ray diffraction analysis was performed using a Burcker D8 Advance diffractometer. The composites density was measured using the Archimedes method (ASTM B962) and compared with theoretical densities to obtain a variable degree of compaction. Elemental analysis of the samples was carried out using wavelength dispersive X-ray spectroscopy (WDS). The samples hardness was measured using the Vickers method at 3 kg load for 10s, and the result was averaged for five readings (standard deviation ±0,31). Moreover, measurements of the softening and melting points were carried out, which were of cognitive character.

The study was carried out using the apparatus and the manner described in the publication [23]. The cylindrical capsule (20×20 mm in size) is formed of material crushed to the extent that it is completely sieved through a sieve with a 0.1 mm square mesh. The binder is an aqueous dextrin solution. This method allows determining three characteristic values:

- T_p – initial softening point,
- T_m – softening point,
- T_t – melting point.

3. Results and discussion

3.1. Composite characterization

Unification of aluminum powder and iron powder during plastic forming by high-temperature extrusion allowed to obtain a composite with high surface quality. It was found that for a composite containing 2% iron, the surface was more favorable and had no defects such as voids, cracks or layered separations. The mechanical properties of extruded bars were tested in a static tensile test [24,25]. The aluminum powder rods obtained after the extrusion process had a tensile strength of 95 MPa, with total elongation of approx. 58%. The introduction of 2% iron powder into aluminum powder resulted in an increase in tensile strength to 144 MPa, however, reducing the elongation to 38%. Comparable plasticity is shown by a composite with 5% added iron powder with an increase in tensile strength up to 149 MPa and a reduction of total elongation by 24% with respect to a composite with 2% iron powder content (Fig. 3).

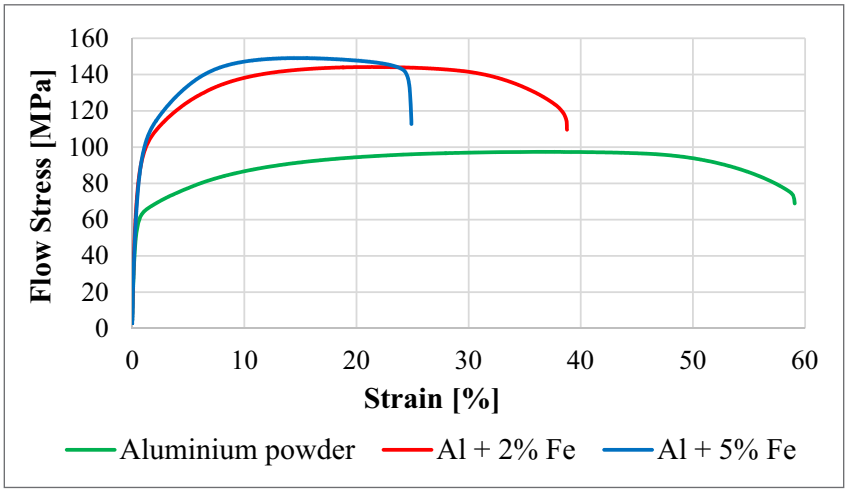

Fig. 3. Graph of the dependence of the yield strength on the deformation of a bar made of aluminum powder, a bar with the addition of 2% and a bar with the addition of 5% iron – One result to all samples were extruded at 400°C

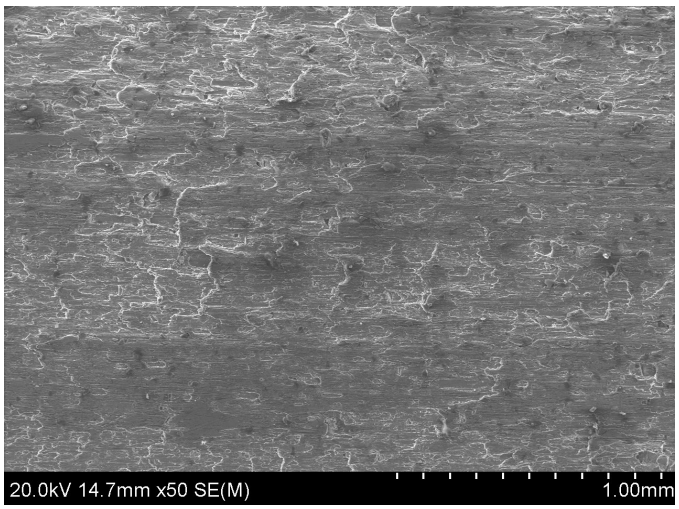

Fig. 4. Surface of the rod based on aluminum with 5% iron powder extruded at 400°C

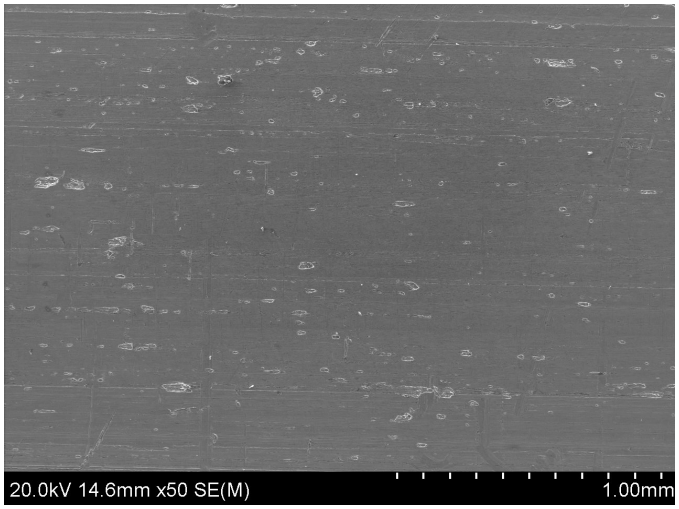

Fig. 5. Surface of the rod based on aluminum with 2% iron powder extruded at 400°C

3.2. Metallographic analysis

Structural analyses carried out at the fracture surfaces of strength samples using the SEM method showed a tendency to increase the porosity as the amount of additive in the form of iron, powder was increased. (Fig. 4 and 5). With respect to porosity, two different types of pores can be observed in composite:

– microstructural pores: residual voids and defects in the microstructure of the built part,
– functional pores: open and connected pores that are caused by debinding; they can be eliminated by HIP or infiltration with polymers or with low-melting point

Fig. 6b and 6c also show the powder's tendency to be well distributed as the iron content increases. Visible spherical agglomerations were identified as iron aggregates (Fig. 7 and 8). The analysis of fractures in the micro-regions (Fig. 7 and 8) has shown incorporation of iron powder agglomerations of about 5-20 micrometers in the center of the compressed aluminum

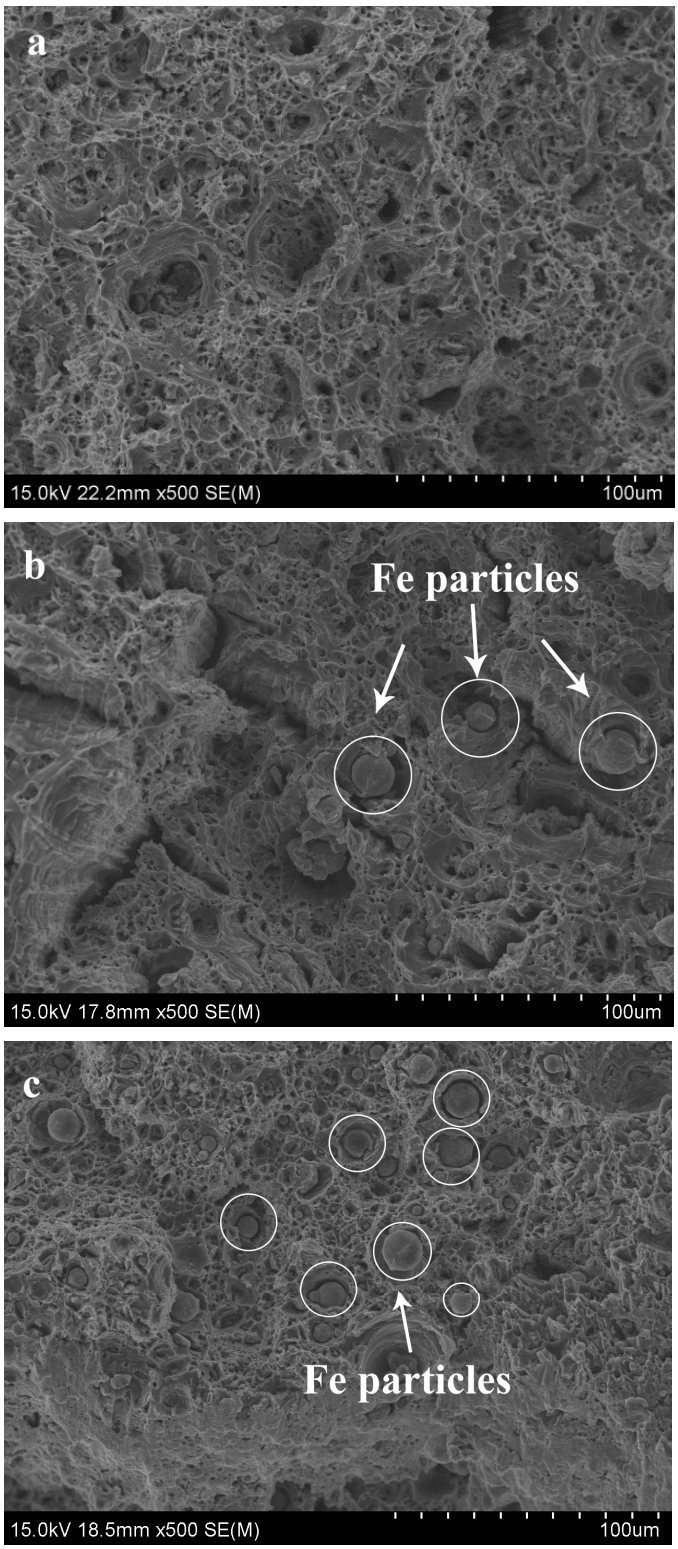

Fig. 6. Topography of the interface (after tensile testing) of a rod extruded from aluminum powder: a) without added iron powder b) with added 2% iron powder c) with added 5% iron powder (500× magnification)

powder structure. In samples containing 5% iron there are more iron aggregates than in those containing 2%, and this amount is proportional to the difference in composition – about twice as many iron agglomerations in a composite containing 5% iron (Fig. 9a). This indicates the lack of solubility of iron in the aluminum powder matrix.

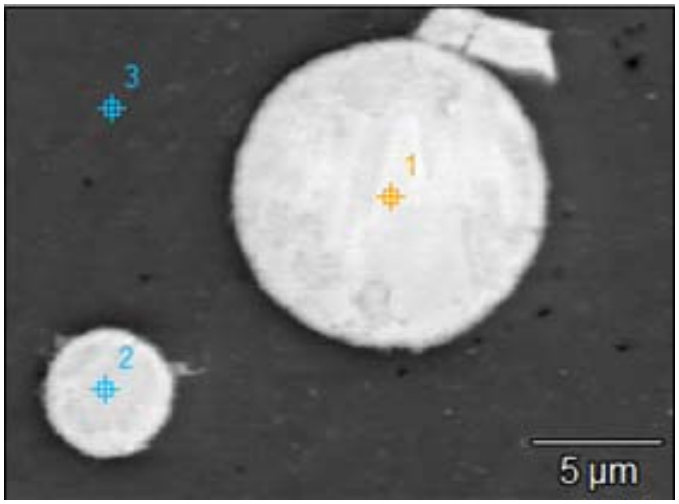

Point No.	Al [wt. %]	Fe [wt. %]
1	1.33	98.67
2	1.45	98.55
3	99.50	0.50

Fig. 7. Results of MRX analysis for a composite with 2% iron content after extrusion

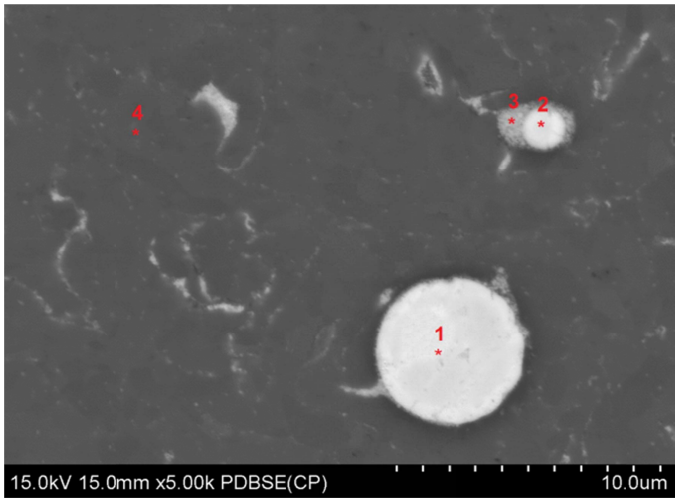

Point No.	Al [wt. %]	Fe [wt. %]
1	1.24	98.76
2	1.45	98.55
3	98.50	1.50
4	99.66	0.34

Fig. 8. Results of MRX analysis for a composite with 5% iron content after extrusion

An additional condition confirming this combination is the accumulation of iron agglomeration, in samples containing 5% iron, along the boundaries of the agglomeration particles (Fig. 9b). For lower iron content (2%), iron secretions are inside the agglomeration particles.

These observations confirm the literature information on low solubility of iron in aluminum – max. 2% [26].

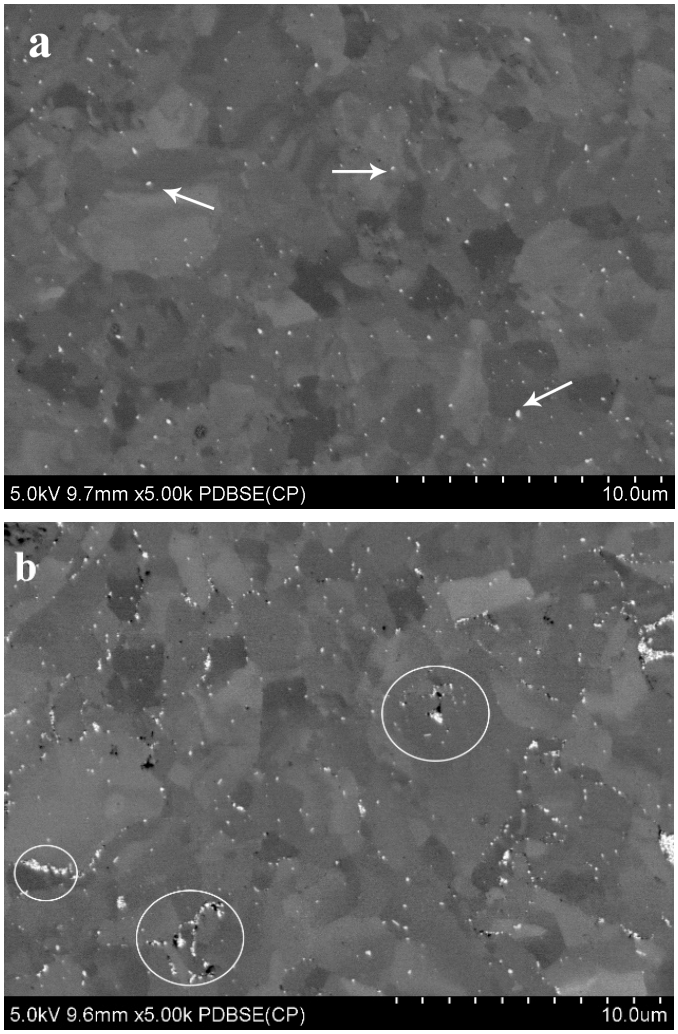

Fig. 9. a) Structural image after extruding composite with 2% iron content, b) Structural image after extruding composite with 5% iron content

3.3. Sintering point

The study used Al-Fe powder with a 2% iron content. The measurement results are shown in Fig. 10. The measurement failed to determine the initial softening point or melting point for both the sample with 2% and 5% iron content. The studied material showed no changes indicating sintering of the composite up to 1330°C, which demonstrates that the composite tested did not sinter up to this temperature. At 1330°C, the sample holder melted slightly and the test was discontinued. The only effect observed is the height of the test capsule increasing by 14%, which could have been caused by the oxygenation of the sample and the formation of a shell on its outer surface. After the measurement, cracks and white coating were also observed on the surface of the capsule. Moreover, upsetting of the capsule was noted (Fig. 11), which may indicate an increase in the volume of the material tested.

The primary issue in the consolidation of aluminum alloys via sintering is the resulting aluminum oxide layer. Despite using shielding gas (argon) during the measurement, insufficient protection of the atmosphere while mixing aluminum powder with iron powder might also have contributed to the oxidation of

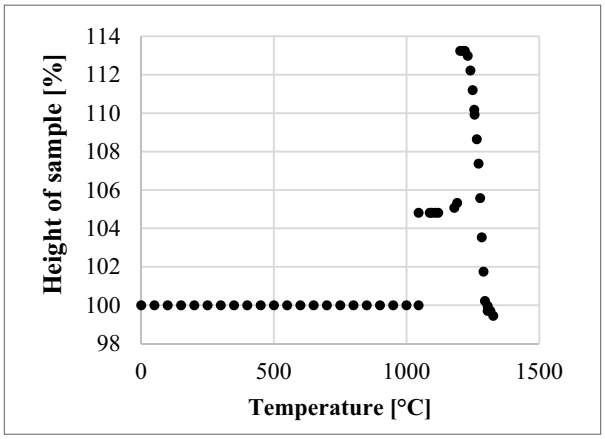

Fig. 10. Change in the height of the tested Al-Fe composite capsule (2% iron powder) due to temperature

3.4. Effect of Fe content on densification

The effect of iron content on densification is shown in Fig. 12. The higher the iron content in the composite, the higher the theoretical density, which can be attributed to a higher Fe density (7.8g/cm^3) than that of pure Al aluminum (2.7g/cm^3). However, sintering the molding at 400°C causes the compaction of aluminum powder, which decreases with an increase of Fe content to the value of 92.3%. This decreasing density results from the agglomeration of iron particles during sintering. The dense network formed by the iron particles during the sintering process prevents further compaction. Moreover, the decrease in compaction is also due to the high Fe hardness (less compressibility), which results in lower compaction.

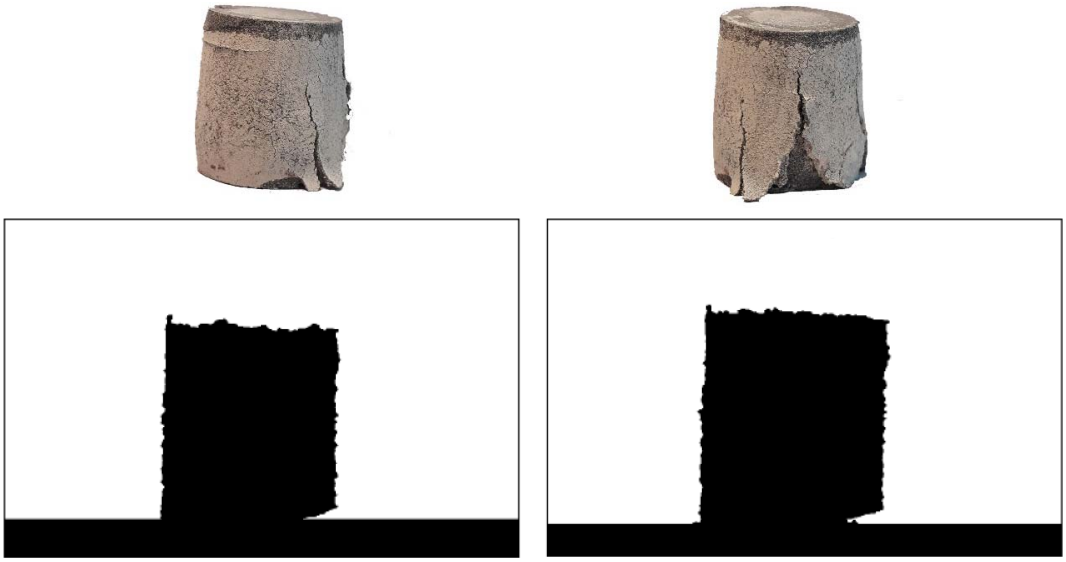

Fig. 11. View of a capsule made of Al-Fe powder (2% iron powder) after measurement

the aluminum powder and thus the composite did not sinter. The thickness of the oxide layer depends on the temperature it formed in and on the atmosphere it is stored in. It usually has a thickness of 10-20 Å [26]. Oxidation of metal can be formulated as:

$$M + 0{,}5\,O_2 = MO \tag{1}$$

The free energy of formation, ΔG, of the oxide is given by:

$$\Delta G = -RT \ln K \tag{2}$$

where R is the gas constant, T the temperature in Kelvin and K the equilibrium constant given by:

$$K = (P_{O_2})^{1/2} \tag{3}$$

where P_{O_2} is the partial pressure of oxygen when reaction (1) is at equilibrium. For aluminum, the partial oxygen pressure at 600°C is $P_{O_2} < 10^{-50}$ atm [27]. Thus, reducing aluminum oxide requires a strongly reducing atmosphere that seems physically unattainable, and therefore aluminum cannot be sintered under conventional laboratory conditions.

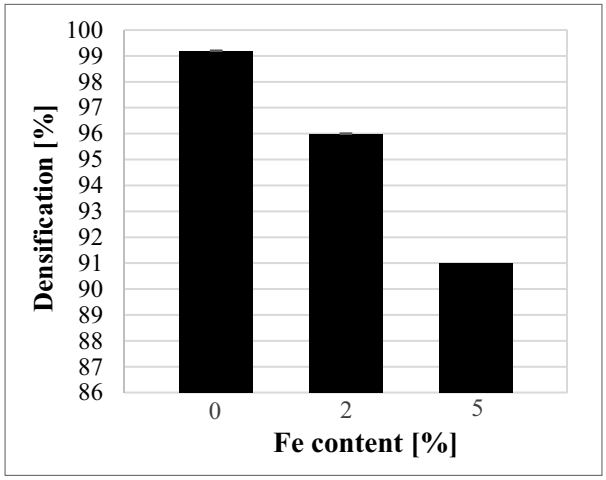

Fig. 12. Bar graph of densification of Al-Fe composites as a function of Fe content

3.5. Effect of Fe content on hardness

The graph illustrating the hardness measured after compaction and sintering of the aluminum powder composite as a function of iron content is shown in Fig. 13. The measured hardness values indicate a continuous increase in hardness with an increase in the Fe content from 0 to 5%. The iron acts in the composite phase as a reinforcing phase that disperses in the aluminum matrix and disrupts displacement in the event of plastic deformation. Intermetallic phases may also be formed in the Al-Fe system [29]. Thus, with the addition of Fe particles, the plasticity of the composite decreases, which can be attributed to the high hardness of Fe. These results are consistent with the results presented in the literature.

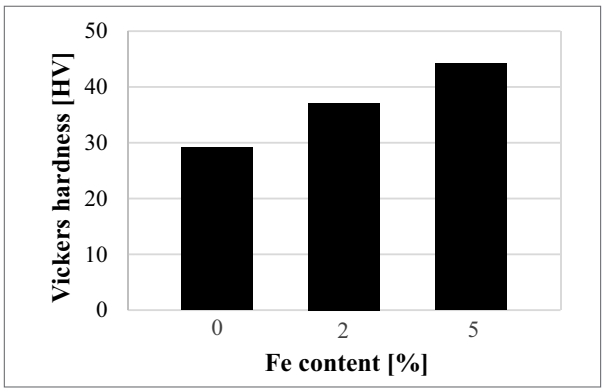

Fig. 13. Bar graph of hardness of Al-Fe composites as a function of Fe content

4. Conclusion

1. The iron powder originated from plasma cutting was successfully introduced into an aluminum powder composite using powder metallurgy.

2. Current research shows that Fe can be distributed in aluminum evenly, and a significant increase in mechanical properties is achieved at the expense of only a slight increase in density.

3. The maximum hardness and tensile strength of a composite with added 5% Fe is: HV 44 and 149 MPa, respectively, which leads to good strength and plasticity of the composite.

4. Determining the sintering point of the powder required a strongly reducing atmosphere ($P_{O2} < 10^{-50}$ atm) which seems virtually unachievable under laboratory conditions, and therefore aluminum cannot be sintered under conventional conditions.

Currently, composite bars can be used to build balcony balustrades in the company on a special order.

REFERENCE

[1] T.T. Sasaki, T. Ohkubo, K. Hono, Acta Mater. **57** (12), 3529-3538 (2009).

[2] I. Adamovich, S. D. Baalrud, A. Bogaerts, A. M. Vardelle, J. Phys. D Appl. Phys. **50** (32), 1-46 (2017).

[3] A. Klimpel, Welding and metal cutting technology **14**, 501-515 (1997).

[4] https://www3.epa.gov/ttn/chief/efdocs/welding.pdf, accessed: 17.10.2019.

[5] DIN EN ISO 9013:2017, Thermisches schneiden – Einteilung thermischer Schnitte – Geometrische Produktspezifikation und Qualitat, 2017 r.

[6] EN ISO 17639:2013-12, Zerstorende Prufung von Schweissverbindung an metallischen Werkstofen – Makroskopische und mikroskopische Untersuchunge von Schweissnahten.

[7] A. Kałasznikow, S. Kłos, Innovations in management and production engineering **1**, 554-563 (2018).

[8] S. Stauss, H. Muneoka, K. Urabe, K. Terashima, Physic of Plasma **22** (5), 1-13 (2015).

[9] Q. Chen, J. Li, Y. Li, J. Phys. D Appl. Phys. **48** (42), 1-25 (2014).

[10] J. Torralba, C.E. Da Costab, F. Velasco, Mater. Process. Technol. **133** (1-2), 203-206 (2003).

[11] J.R. Pickens, J. Mater. Sci. **16,** 1437-1457(1981).

[12] Y.B. Liu, S.C. Lim, L. Lu, M.O. Lai, J. Mater. Sci. **29** (8), 1999-2007 (1994).

[13] B. Huang, N. Tokizane, K.N. Ishihara, P.H. Shingu, S. Nasu, J. Non-Cryst. Solids **117-118** (2), 688-691 (1990).

[14] D.K. Mukhopadhyay, C. Suryanarayana, F.H. Froes, Metall. Mater. Trans. A **26** (8), 1939-1946 (1995).

[15] B.S. Murty, S. Ranganathan, Int. Mater. Rev. **43** (3), 101-141 (1998).

[16] K.N. Ishihara, F. Kubo, E. Yamasue, and H. Okumura, Rev. Adv. Mater. Sci. **18** (3), 284 (2008).

[17] E. Bayraktar, D. Katundi, J. Achiev. Mater. Manuf. Eng. **38**, 7-14 (2010).

[18] A. Mazahery, M.O. Shabani, Ceram Int. **38** (5), 4263-4269 (2012).

[19] A. Mazahery, M.O. Shabani, Powder Technol. **217**, 558-565 (2012)**.**

[20] A. Fathy, O. El-Kady, M.M. Mohammed, Trans. Nonferrous Met. Soc. China **25**, 46-53 (2015).

[21] A.K. Kaw (Ed.), Mechanics of composite materials, 2nd ed., Taylor & Francis Group, New York (2006).

[22] G.E. Dieter (Ed.), Mechanical Metallurgy: Principles and Applications 3rd ed., McGraw-Hill, New York (1976).

[23] A. Zajączkowski, J. Norwisz, J. Botor, Non-ferrous Ores and Metals **31**, 275-277 (1986).

[24] G. Włoch, T. Skrzekut, J. Sobota, A. Woźnicki, J. Cisoń, Key Eng. Mater. **682**, 245-251 (2016).

[25] T. Skrzekut, A. Kula, L. Błaż, Key Eng. Mater. **682**, 259-264 (2016).

[26] W. Khraisat, J. Abu Jadayil, J. Mech. Ind. Eng. Res. **4** (3), 372-377 (2010).

[27] E.M. Ruiz-Navas, M.L. Delgado, J.M. Torralba, Adv. Mat. Res. **23**, 51-58 (2007).

[28] M. Qian, G.B Shaffer, Sintering of aluminium and its alloys, in: Zhigang Zak Fang (Ed.), Sintering of Advanced Materials (2010), Woodhead Pulblishing (2010).

[29] X. Li, A. Scherf, M. Hellmaier, F. Stein, J. Phase Equilib. Diffus **3**, 162-164 (2016).